



## **Synthesis of cationic quaternized pullulan derivatives for miRNA delivery.**

Fernanda Moraes, Joana Antunes, Laura Marcela Forero Ramirez, Paola Aprile, Gregory Franck, Cédric Chauvierre, Frédéric Chaubet, Didier Letourneur

### **► To cite this version:**

Fernanda Moraes, Joana Antunes, Laura Marcela Forero Ramirez, Paola Aprile, Gregory Franck, et al.. Synthesis of cationic quaternized pullulan derivatives for miRNA delivery.. International Journal of Pharmaceutics, 2020, 577, pp.119041. <10.1016/j.ijpharm.2020.119041>. <hal-03022444>

**HAL Id: hal-03022444**

**<https://hal.science/hal-03022444v1>**

Submitted on 21 Jul 2022

**HAL** is a multi-disciplinary open access archive for the deposit and dissemination of scientific research documents, whether they are published or not. The documents may come from teaching and research institutions in France or abroad, or from public or private research centers.

L'archive ouverte pluridisciplinaire **HAL**, est destinée au dépôt et à la diffusion de documents scientifiques de niveau recherche, publiés ou non, émanant des établissements d'enseignement et de recherche français ou étrangers, des laboratoires publics ou privés.



Distributed under a Creative Commons CC BY-NC 4.0 - Attribution - Non-commercial use - International License

# Synthesis of cationic quaternized pullulan derivatives for miRNA delivery

Fernanda C. Moraes <sup>a, \*</sup>, Joana C. Antunes <sup>b</sup>, Laura Marcela Forero Ramirez <sup>a</sup>, Paola Aprile <sup>a</sup>,  
Gregory Franck <sup>a</sup>, Cédric Chauvierre <sup>a, §</sup>, Frédéric Chaubet <sup>a, §</sup>, Didier Letourneur <sup>a</sup>

- 5 a) Université de Paris, LVTS, INSERM U1148, Université Paris 13, F-75018 Paris, France;  
fernanda.moraes@inserm.fr; lmforeror@gmail.com; paola.aprile@inserm.fr; gregory.franck@inserm.fr;  
cedric.chauvierre@inserm.fr; fchaubet@gmail.com; didier.letourneur@inserm.fr  
b) Universidade do Minho, 2C2T, Campus de Azurém, 4800-058 Guimarães, Portugal;  
joana.antunes@2c2t.uminho.pt

## 10 § Equivalent work

\*Correspondence: fernanda.moraes@inserm.fr; Tel.: + 33 07 62 32 23 73

**Abstract:** Pullulan is a natural polysaccharide of potential interest for biomedical applications due to its non-toxic, non-immunogenic and biodegradable properties. The aim of this work was to synthesize cationic pullulan derivatives to be able to form complexes with microRNAs (miRNAs) driven by electrostatic interaction (polyplexes). Quaternized ammonium groups were linked to pullulan backbone by adding the reactive glycidyltrimethylammonium chloride (GTMAC). The presence of these cationic groups within the pullulan was confirmed by elemental analysis, Fourier-transform infrared spectroscopy (FTIR) and proton nuclear magnetic resonance (<sup>1</sup>H-NMR). The alkylated pullulan was able to interact with miRNA and form stable polyplexes that were characterized regarding size, zeta potential and morphology. The presence of miRNA was confirmed by agarose gel electrophoresis and UV spectrophotometry. *In vitro* tests on human umbilical vein endothelial cells did not show any cytotoxicity after 1 day of incubation with nanosized polyplexes up to 200 µg/mL. QA-pullulan was able to promote miRNA delivery inside cells as demonstrated by fluorescence microscopy images of labelled miRNA. In conclusion, the formation of polyplexes using cationic derivatives of pullulan with miRNA provided an easy and versatile method for polysaccharide nanoparticle production in aqueous media and could be a new promising platform for gene delivery.

**Keywords:** pullulan; cationic derivatives; polyplexes; microRNA; gene therapy

*Abbreviations:* miRNA, MicroRNA; ncRNAs, small Non Coding RNAs; pDNA, Plasmid DNA; PEI, Polyethyleneimine; PAMAM Polyamidoamine; siRNA, small interfering RNA; QA-pullulan, Quaternized ammonium- pullulan; Mw, Weight average molecular weight; Mn, Number average molecular weight; GTMAC, Glycidyltrimethylammonium chloride; 6-FAM, 6-Fluorescein amidite; SEC-MALLS, Size exclusion chromatography- multiangle laser light scattering; FTIR, Fourier-transform infrared spectroscopy; <sup>1</sup>H-NMR, Proton nuclear magnetic resonance; TBE, Tris-Borate-EDTA; Pdl, Polydispersity Index; HUVECs, Human umbilical vein endothelial cells; PBS, Phosphate buffered saline; DS, Degree of substitution; AGU, Anhydroglucose unit; DAPI, 4',6-Diamidino-2-phenylindole; TPP, tripolyphosphate; kcps, kilo counts per second.

## 1. Introduction

Gene therapy uses nucleic acids (DNA or RNA) for the treatment, cure or prevention of human disorders by the insertion of new genes into target cells (Cao et al., 2019). The use of nucleic acids as drugs has been described for two decades (Wolff JA et al., 1990), being mainly based on viral vectors and plasmid DNA technology (Xiong et al., 2018; Zarghampoor et al., 2019). More recently, small non coding RNAs (ncRNAs), namely microRNAs (miRNAs), have emerged as key regulators of gene expression as a promising alternative to conventional plasmid DNA (pDNA) due to its multiple unique features and advantages when compared to DNA-based therapy (Bernardo et al., 2015; Xiong et al., 2018).

miRNAs are small endogenous single stranded non-coding RNA molecules that play important roles in many cellular processes such as cell differentiation, proliferation and survival acting on post-transcriptional level by binding to complementary target mRNAs, resulting in mRNA translational inhibition or degradation (Rupaimoole and Slack, 2017). miRNAs have been proposed and investigated as therapeutics and biomarkers for various diseases such as cancer, diabetes, cardiovascular diseases and other pathologies whose etiology is related to aberrant gene expression (Candido et al., 2019; Falzone et al., 2019; Gaur et al., 2015; Hou et al., 2012; Poddar et al., 2019; Zhu et al., 2019). At the target, miRNAs can generate strong, sustained and comprehensive biological effects, through endogenous gene silencing with very low concentrations (at least 0.5 nM) (Devaux et al., 2015; Qiagen, 2018). Additionally, miRNAs are able to affect multiple pathways/cellular processes rather than specific targets (van Rooij et al., 2008). The success of miRNA-based therapies depends

on the development of suitable vehicles able to specifically target cells for the efficient delivery of the nucleic acids, with minimum toxicity (Chakraborty et al., 2017).

60 Compared to DNA-based gene therapy, the delivery of miRNA is more challenging due to important differences in terms of size and structure. Most of the polymeric delivery strategies originally developed for plasmid DNA (pDNA) in gene therapy cannot be used for miRNA delivery without formulation optimization since miRNA are much smaller molecules (21-23 bp) than DNA (several kilo bp). Thereby, small RNAs are more difficult to be packaged and condensed into stable  
65 systems for protection against early clearance and degradation (Nuhn et al., 2014; Scholz and Wagner, 2012). Moreover, the vulnerability of RNA to enzymatic degradation (hydrolyses) by serum nucleases due to an extra hydroxyl group in the 2' position of pentose ring in ribose structure, instead of a hydrogen atom present in DNA structure, induced additional challenges to RNA delivery (Gary et al., 2007; Mao et al., 2010).

70 Several types of biomaterials have been used as platforms for gene delivery, and in particular positively-charged polymers represent a high proportion. They can bind nucleic acids via electrostatic interactions to form particulate structures named polyplexes (Shen et al., 2017). Polyplexes are formed in solution by the direct mixing of two oppositely charged polyelectrolytes and the main driving force that guides polyplex formation is an increase in the entropy of the system due to the release of  
75 low-molecular weight counterions which is able to produce nanoparticles containing the nucleic acid payload in a compacted and protected structure (Lächelt and Wagner, 2015; Lounis et al., 2016). The easy manipulation and versatility of physicochemical properties are some of the most important advantages of polymeric gene carriers (Patil et al., 2005).

Cationic polymers that have been used for the delivery of miRNAs include polyethyleneimine  
80 (PEI), polyamidoamine (PAMAM) dendrimers and chitosan (Mao et al., 2010; Scholz and Wagner, 2012). Polymers derived from natural sources could be preferable in gene therapy applications because they are naturally biocompatible, biodegradable and nontoxic and can overcome the cytotoxicity associated with the use of several synthetic polymers which does not satisfy the requirements for clinical applications. However, cationic chitosan, one of the most studied polymers  
85 of the list, has its own drawbacks such as low water solubility at physiological pH because of partial protonation of primary amino groups which can affect nucleic acid interactions and stability of complexes in bloodstream (Gary et al., 2007; Ragelle et al., 2014). Thus, the design of biocompatible, stable and efficient nanocarriers is needed (Shi et al., 2017). In contrast to the large amount of

synthetic non-viral gene delivery systems, there is only a small number of polycations of natural origin  
(Thanou et al., 2002).

Pullulan is a natural polysaccharide derived from *Aureobasidium pullulans* that consists of maltotriose units and due to its non-toxic, non-immunogenic and biodegradable properties, is considered as a promising material for biomedical applications (K.R. and V., 2017). It is admitted safe in the United States for a wide range of applications, such as an excipient in pharmaceutical tablets and listed in the Japanese Standards as accepted adjuvant for drug delivery (Prajapati et al., 2013; Rekha and Sharma, 2009). Cationic pullulan derivatives grafted with primary or tertiary amine groups were previously demonstrated to be able to form complexes with plasmid DNA as well as siRNA in cationized pullulan-based hydrogels (San Juan et al., 2009, 2007). However, the ionic interaction between the macromolecules closely depend on the pH. Hydroxyl groups of pullulan can be easily substituted with quaternized ammonium groups (QA) to improve the interaction with negatively charged nucleic acids (San Juan et al., 2007; Shao et al., 2014). QA derivatives are an interesting strategy for gene therapy due to their permanent positive charges independent of the pH (Ahmed and Aljaeid, 2016). In this work, polycations have been obtained by grafting QA using glycidyltrimethylammonium chloride at different feeding ratios into the pullulan backbone. Then, QA-pullulan formulations were used to form nanosized polyplexes with miRNAs opening the way to their use as a platform for gene delivery.

## 2. Materials and Methods

### 2.1 Materials

Pullulan (Mw 200 kg/mol) was purchased from Hayashibara Company (Okayama, Japan). Glycidyltrimethylammonium chloride (GTMAC) (Mw 151.63 g/mol) was purchased from Sigma-Aldrich (St. Louis, MO, USA). Dialysis membranes of 20 kDa was purchased from Spectrum Laboratories (New Brunswick, NJ, USA). Single-stranded miRNA and 6-Fluorescein AMidite (6-FAM)-miRNA scramble oligonucleotides with 23 bp of length (RNA sequence: 5'-UUA AUG CUA AUC GUG AUA GGG GU-3') used to mimic the natural human mature microRNA miR-155-5p were purchased from Sigma-Aldrich (Saint Quentin Fallavier, France). Sequence was reconstituted in RNase-free water to achieve a final concentration of 20  $\mu$ M and stock solutions were stored at -20°C. Ultrapure water was prepared by ion-exchange of running tap water (Millipore, France).

## 2.2 Synthesis of cationized pullulan

### 2.2.1 Alkylation with GTMAC

120 Pullulan was synthesized based on a protocol previously described by San Juan *et al.* to graft  
primary and tertiary amine groups into pullulan backbone (San Juan *et al.*, 2007). Briefly, pullulan (500  
mg) was dissolved in 5 mL of an aqueous solution of 10 M NaOH. Then, the solution was placed at 4°C  
under magnetic stirring until pullulan was completely solubilized. Glycidyltrimethylammonium chloride  
(GTMAC) was added to polysaccharide solution at different feeding ratios (1 eq = 3.1 mmol; 2 eq = 6.2  
125 mmol, and 3 eq = 9.3 mmol) drop by drop and under high magnetic stirring at 4°C. The solution was  
placed under magnetic stirring at 55°C for 4 hours. After cooling down to room temperature, the pH was  
adjusted to 7 with concentrated hydrochloric acid solution. The mixture was exhaustively dialyzed  
(MWCO of 20 kDa) for 48 hours with ultrapure water and the derivatives were obtained as fluffy white  
materials after freeze-drying.

## 130 2.3 Chemical characterization of modified pullulan

### 2.3.1 Elemental analysis

Elemental analysis (C, H, N, O) was performed by the Microanalysis service of *Centre National de  
la Recherche Scientifique* (CNRS) (Gif/Yvette, France) (Table 1 and Table A.1). Degree of substitution  
was estimated using N content values.

### 135 2.3.2 Molecular weight determination

Weight-average molecular weight ( $M_w$ ) and number-average molecular weight ( $M_n$ ) were  
determined by size exclusion chromatography (SEC) coupled to a multiangle laser light scattering  
(MALLS) detector (DAWN-F, Wyatt Technology, Santa Barbara, CA, USA). The SEC line consisted of a  
TSK-Gel PWXL Guardcolumn and TSK-Gel GMPWXL in series (Tosoh Bioscience, Stuttgart,  
140 Germany). The eluent was 0.2 M  $\text{NaNO}_3$  containing 0.02% (w/v)  $\text{NaN}_3$  at 0.5 mL/min flow rate. The  
samples were dissolved in the eluent at a concentration of 10 mg/mL. The  $dn/dc$  value used for the  
molecular weight distribution calculations was 0.14. The collected data were analyzed using the  
software Astra V-6.1.2 (Santa Barbara, CA).

### 2.3.3 FTIR spectroscopy

145 FTIR spectroscopy was carried out with KBr pellets on a Thermo-Nicolet-AVATAR 370 FTIR (Thermo Electron Corporation, Waltham, MA). A first pellet with 200 mg of KBr was prepared. Then, pellets were made using 200 mg KBr and 2 mg of polymer. A 32-scan interferogram was collected in transmittance mode. Scans were taken from 400  $\text{cm}^{-1}$  to 4000  $\text{cm}^{-1}$  at a resolution of 2  $\text{cm}^{-1}$ . The spectrum of KBr pellet was used as background.

#### 150 2.3.4 NMR spectroscopy

$^1\text{H}$ -NMR spectra was recorded with a Bruker-400 Ultrashield (Bruker, Germany) operating at 400 MHz. Polymers samples were prepared in  $\text{D}_2\text{O}$  at a concentration of 20 mg/mL.

### 2.4 Synthesis of QA-pullulan/miRNA Polyplexes

Briefly, cationic pullulan and anionic miRNA were dissolved in ultrapure water to obtain stock  
155 solutions at 0.08 mg/mL and 0.04 mg/mL, respectively. All polysaccharide solutions were filtered before use (0.2  $\mu\text{m}$ ). Nanosized polyplexes were produced by dropping 1 mL of miRNA solution over 1 mL of quaternized pullulan solution under high magnetic stirring at room temperature in aqueous solution. Samples were placed at 4°C during 20 min for stabilization before use.

### 2.5 Characterization of QA-pullulan/miRNA Polyplexes

#### 160 2.5.1 Size and zeta potential measurements

Particle size and zeta potential of polyplexes were measured by Dynamic Light Scattering (DLS) and Electrophoretic Light Scattering (ELS) using a Zetasizer Nano-ZS (Malvern Instruments, Malvern, UK) respectively. Size and zeta potential measurements were performed at 25°C using a 173° and 13° scattering angle for size and zeta potential measurements, respectively, equipped with a 4 mW HeNe  
165 laser beam with a wavelength of 633 nm. Size and  $\zeta$  potential values were automatically calculated through the software DTS Nano v.6.30 (Malvern, UK) using the Stokes-Einstein equation and the Henry equation with the Smoluchowski approximation, respectively. Size measurements were performed in water using disposable polystyrene cuvettes and zeta potential measurements were performed in 1 mM KCl solution using a DTS1070-folded capillary cell (ELS, Malvern, UK). Data were acquired in triplicate.

#### 170 2.5.2 Morphology

The morphology of optimized polyplexes was assessed using a Transmission Electron Microscope (TEM) Tecnai 12 (80 kV; FEI; Hillsboro, OR, USA) with a 1K x 1K KeenView camera (OSiS). Nanosized polyplexes were produced as previously described. Then, 3  $\mu$ L of polyplexes suspension was placed onto a 400  $\mu$ L mesh copper grid coated with carbon (EMS) without any sample dilution. Uranyl acetate 1% (w/v) was used for negative staining. TEM pictures was performed at the platform ImagoSeine of the Institute Jacques Monod (Paris, France).

### 2.5.3 miRNA presence into polyplexes

The presence of the miRNA was monitored by agarose gel electrophoresis (AGE) and UV spectrophotometry after miRNA desorption. Agarose gel electrophoresis was performed using 5% agarose gels containing ethidium bromide in TBE (Tris-Borate-EDTA, Thermo Fisher Scientific, Vilnius, Lithuania) buffer. An Ultra-Low Range GeneRuler DNA Ladder (10-300 bp; Thermo Fisher Scientific, Bleiswijk, Netherlands) was used to monitor miRNA presence. Samples included solution of free polymer (QA-pullulan), plus additional controls from different steps of the miRNA loading: miRNA alone (at the concentration used for loading), QA-pullulan polysaccharide solution and QA-pullulan/miRNA polyplexes. Samples were run by electrophoresis (50 V, 120 min) and detected through a UV transilluminator (Vilber Lourmat smart imaging system, Collegien, France). Additional miRNA quantification was performed by UV spectrophotometry using NanoDrop™ 2000/2000c Spectrophotometer (Thermo Fisher Scientific, Wilmington, DE, USA).

### 2.5.4 Stability of QA-pullulan/miRNA Polyplexes

The stability of complexes was evaluated over time while stored at 4°C in aqueous media. Size and Pdl (Polydispersity Index) evolutions of polyplexes suspensions were monitored by DLS (n= 3) at each time point (0h, 6h, 12h, 18h, 24h).

### 2.5.5 Cytotoxicity of QA-pullulan and QA-pullulan/miRNA Polyplexes

Cytotoxicity was evaluated in Human Umbilical Vein Endothelial Cells (HUVECs, ATCC CRL-1730, Manassas, VA, USA) by resazurin conversion assay (Sigma-Aldrich, Saint Louis, MO, USA). Cells were seeded at a concentration of 10,000 cells/well onto 96-well plates in Dulbecco's Modified Eagle Medium (DMEM) (Thermo Fisher Scientific, Carlsbad, CA, USA) supplemented with 10% (v/v) of fetal bovine serum, 1% (v/v) of penicillin and 1% (v/v) of streptomycin in a humidified



atmosphere with 5% CO<sub>2</sub> at 37°C. At a subconfluent to confluent stage, cells were detached with 0.05% trypsin/EDTA (Gibco) and re-seeded until the required number of cells for the subsequent experiments was obtained. Cell metabolic activity was assessed after different culture conditions by resazurin conversion. Cells were incubated with medium containing 10% resazurin for 2 hours at 37°C. Fluorescence intensity (530 nm/590 nm) of the cell culture supernatants was measured with an Infinite® PRO microplate reader (TECAN Group Ltd., Männedorf, Switzerland). A blank control comprising only medium was also included. Bright field images (EVOS™ XL Core Cell Imaging System, Thermo Fisher Scientific, Carlsbad, CA, USA) were taken during culture to monitor cell morphology.

#### 2.5.6 miRNA delivery

Human Umbilical Vein Endothelial Cells (HUVECs, ATCC CRL-1730, Manassas, VA, USA) cells were seeded at a concentration of 8,000 cells/well onto Nunc™ Lab-Tek™ chamber slides (Thermo Fisher Scientific) and grown for 48 hours. Polyplexes of QA-pullulan and scramble FAM-miRNA were prepared as previously described on the same day of treatment and incubated for 20 min at 4°C before adding to the cells. After 30 min of incubation using serum-free supplemented cell culture medium, cells were washed with PBS and fixed with fresh 4% paraformaldehyde. Cell nucleus was stained with 4',6-DiAmidino-2-PhenylIndole (DAPI) (Sigma Aldrich, St. Louis, MO, USA). Coverslips were mounted using Ibbidi Mounting Medium (IMM) for fluorescence microscopy (ibidi GmbH, Germany). Fluorescence images were taken to evaluate miRNA delivery (Axiovert Observer Z1 inverted microscope, Zeiss, Germany).

#### 2.6 Statistical analysis

The data were expressed as mean ± SD (standard deviation). Statistical analysis was performed using GraphPad Prism (version: 5.0a, San Diego, CA, USA). Since data followed a non-parametric distribution, Wilcoxon matched-pairs test was performed to compare each paired group and p smaller than 0.05 was considered to be statistically significant.

### 3. Results and discussion

#### 3.1 Chemical modification of pullulan and characterization

Pullulan was grafted with glycidyltrimethylammonium chloride to give QA groups (Figure 1) with molar feeding ratios of 1, 2 and 3 to get QA-pullulan. Cationic derivatives were characterized to

confirm the success of incorporation of trimethylammonium groups into the pullulan backbone. Nitrogen elemental analysis confirmed the substitution reaction with N content ranging from 1.8 to 3.3% (w/w) corresponding to 1.3 to 2.3 mmol of QA groups per g of polymer. SEC-MALLS analysis evidenced monomodal molecular weight distributions (Pdl ranging from 1.1 to 1.4) (Table 1 and Table A.1).

**Table 1.** Characterization of pullulan and cationic pullulan derivatives.

Amine	Feeding <sup>a</sup>	M <sub>n</sub> <sup>b,c</sup> (kDa)	M <sub>w</sub> <sup>b,c</sup> (kDa)	Pdl <sup>b</sup>	N <sup>d</sup> (%)	DS <sup>e</sup>
No amine (pullulan)	0	113	298	2.6	0	0
QA-pullulan	1	125	186	1.4	1.83 ± 0.25	0.3
	2	240	270	1.1	2.75 ± 0.34	0.4
	3	275	320	1.2	3.27 ± 0.04	0.5

<sup>a</sup>Feeding: mol<sub>amine</sub>/mol<sub>hydroxyl groups</sub>, <sup>b</sup>Measured by SEC-MALLS, <sup>c</sup>SD ± 5-10%, <sup>d</sup>From nitrogen elemental analysis,

<sup>e</sup>Degree of substitution of QA-pullulan calculated per anhydroglucose unit.

**Table A.1.** Elemental analysis of pullulan and cationic pullulan derivatives.

Amine	Feeding <sup>a</sup>	N (%)	C (%)	H (%)	O (%)
No amine (pullulan)	0	Absence	41.92 ± 0.06	6.35 ± 0.01	51.88 ± 0.11
QA-pullulan	1	1.83 ± 0.25	42.52 ± 0.34	7.09 ± 0.06	46.99 ± 0.55
	2	2.75 ± 0.34	41.88 ± 0.43	7.27 ± 0.19	44.04 ± 0.91
	3	3.27 ± 0.04	43.40 ± 0.14	7.49 ± 0.09	43.26 ± 0.07

<sup>a</sup>Feeding: mol<sub>amine</sub>/mol<sub>hydroxyl groups</sub>

The extent of the derivatisation reaction was given by the degree of substitution (DS) defined as the number of substituted hydroxyls groups per AGU (AnhydroGlucose Unit) (Cumpstey, 2013). DS can be calculated using N content from elemental analysis results. Derivatives with a degree of substitution in QA groups around 0.3-0.5 were obtained in one step and in a shorter time (4 hours) compared to others protocols used to obtain quaternized polymers with reaction time of 8, 14 and 24 hours (Dionísio et al., 2016; Liu et al., 2015; Stefan et al., 2016). Moreover, the protocol of Liu *et al.* performed in 8h used a mixture of water and isopropanol as reaction medium contrary to our protocol performed only in water without organic solvent (Liu et al., 2015).

IR spectra of pullulan and its cationic derivative presented the general pattern characteristic of polysaccharides (Stuart, 2004). The substitution with QA groups was confirmed by a signal at 1470 cm<sup>-1</sup> (Figure 2) due to C-H scissoring in methyl groups (Li et al., 2016; Stefan et al., 2016). This was

further confirmed by <sup>1</sup>H-NMR spectra (Figure 3) with signals at 3.2 ppm and 4.4 ppm (Dionísio et al., 2016; Stefan et al., 2016).

Highly charged cationic polymers can have non-specific interactions with polyanionic biomolecules in the bloodstream leading to the inhibition of many crucial cellular processes and causing severe inflammatory reactions (Rekha and Sharma, 2009; Shi et al., 2017). When compared to non-modified pullulan, cationic pullulan did not show toxicity up to 72h of incubation with increasing concentrations of QA-pullulan until 1,000 µg/mL (Figure 4) and supports results of literature that pullulan modified with glycidyltrimethylammonium chloride is a nontoxic polymer (Stefan et al., 2016).

### 3.2 Synthesis and characterization of QA-pullulan/miRNA Polyplexes

Polyplexes were prepared by mixing miRNA and QA-pullulan at different concentrations under strong magnetic stirring (Figure 5). They were incubated at 4°C for 20 minutes for stabilization of complexes before use. Once QA-pullulan modified with only 1.83% of N showed to be able to form complexes with miRNA by electrostatic interactions, this derivative was selected for all further optimizations. To optimize the production of stable polyplexes, a fixed concentration of miRNA of 5 nmol (0.04 mg/mL) was selected based on previous works performed by Antunes *et al.* 2019 (Antunes et al., 2019). Different N/P ratios (0.5-15) were tested by increasing the concentration of QA-pullulan. All physicochemical characterizations are summarized in Figure 6. Samples were characterized by DLS/ELS regarding size, Pdl and zeta potential values (Figure 6C). Complexes were formed at an optimized N/P molar ratio of 0.8 producing polyplexes in the nanosized range with a diameter around 130 ± 30 nm and narrow distribution as shown by the polydispersity index (0.07 ± 0.04). More negative zeta potential values of QA-pullulan/miRNA polyplexes (-12 ± 5 mV) as compared to zeta potential of cationic pullulan solution alone (31 ± 6 mV), suggested the presence of additional negative charges at the surface due to miRNA presence in the complex. The morphology of complexes was characterized by TEM (Figure 6B) evidencing the formation of homogeneous spherical particles. The observed sizes were well-correlated with those determined by DLS. miRNA presence was confirmed by agarose gel electrophoresis by the presence of a band in the expected region of 23 bp after miRNA desorption from QA-pullulan (Figure 7A). miRNA was quantified using the software ImageJ by the intensity of the band of polyplexes in the agarose gel normalized by the control naked miRNA and the loading efficiency was around 80%. There was no miRNA degradation or fragmentation after loading as suggested by the absence of smeared bands in AGE indicating that

280 QA-pullulan could effectively protected miRNA. Further miRNA quantification by UV spectrophotometry (Figure 7B) displayed a similar trend as in AGE results.

The N/P ratio, which corresponds to the ratio between QA groups of pullulan derivatives to the phosphate groups of nucleic acid, plays an important role in the capacity of complexation, particle diameter, stability and cytotoxicity of carriers (Tekie et al., 2015; Vauthier et al., 2013; Zhao et al., 285 2009). Generally, polyplexes can be formed between polycations and nucleic acids at relatively low N/P ratios (Shao et al., 2014). In our case, this optimum was found at N/P of 0.8. Furthermore, it was described that an increase in the average molecular weight ( $M_n$ ) of polymer dramatically improved oligonucleotides encapsulation at low N/P ratios (Ahmed and Aljaeid, 2016; de Paula Pansani Oliveira et al., 2013; Vauthier et al., 2013). In a study of Liu and co-workers chitosan with chains 290 having 5 to 10 times the length of siRNA (i.e. with a molecular weight ranging from 65 to 170 kDa) were most suitable to form stable complexes (Liu et al., 2007). Further studies could investigate the effect of the molecular weight of pullulan and its consequence in terms of both physicochemical characteristics of the polyplexes and *in vivo* biodistribution/biodegradation.

Stability of complexes in aqueous media was evaluated here under storage at 4°C over 1 day 295 without forming aggregates (Figure 8). In addition, it is noteworthy that our method of complex formation was developed without the use of any chemical crosslinking agent.

The increase of the ionic strength has a significant impact on colloidal stability with aggregate formation, and higher Pdl values correlated with the heterogeneity of complexes in this medium. Alameh *et al.* described that the colloidal instability in 150 mM NaCl increased with the increase of 300 molecular weight when comparing chitosan with low (10 kDa) and high (120 kDa)  $M_n$  (Alameh et al., 2018). Keeping a good stability in physiological conditions is one of the major challenges when designing vectors intended for intravenous administration (Ragelle et al., 2014). To achieve this goal, several strategies were thought to overcome this limitation and improve stability in biological fluids (Mao et al., 2010). A classical strategy uses cross-linkers such as sodium tripolyphosphate (TPP) for 305 the preparation of chitosan NPs with nucleic acids (Karimi et al., 2013; Wang et al., 2015). However, TPP is a chemical agent with limited sites of interaction for ionotropic gelation (Avadi et al., 2010). Hence, the colloidal stability of polyplexes nanosystems in physiological conditions was far from being fully addressed in the previous investigations (Wu and Delair, 2015).

To assess if the developed polyplexes could be used in biomedical applications, namely as 310 vectors for gene therapy, the cytocompatibility towards HUVECs was evaluated here through an *in*

*vitro* toxicological assay based on resazurin conversion. *In vitro* tests did not evidence any toxic effect of the QA-pullulan/miRNA complexes after 1 day of incubation up to the maximum tested dose of 200 µg/mL of polyplexes (n=3) (Figure 9A). We did not observe any alteration in cell morphology (Figure 9B). This important result is a key aspect to further investigate the potential use of the new biocompatible systems.

Finally, a comparative study of free miRNA, neutral pullulan/miRNA and polyplexes of QA-pullulan/miRNA, was done using a fluorescently labeled miRNA to evaluate their cellular uptake. As it can be seen from Figures 10B and 10C, no miRNA could be detected inside cells in case of administration of free miRNA or unmodified pullulan and miRNA indicating that free miRNA could hardly be internalized by cells. miRNA from polyplexes, in contrast, was clearly incorporated by cells (Figure 10D) by forming complexes with QA-pullulan that is able to promote their internalization usually via endocytic pathways being 150 nm the accepted size limit for cellular uptake by non-specific endocytosis (Ganas et al., 2014; Gary et al., 2007; Goyal et al., 2018).

#### 4. Conclusions

This work demonstrated that nanosized polyplexes are formed and are stable in aqueous medium by simply mixing miRNA with pullulan substituted with quaternized ammonium groups. Such pullulan derivatives have been previously used by André and co-workers to modify the surface of nanoparticles based on sorbitan monooleate (Span® 80) in order to increase the interaction of this system with siRNA for cellular therapy (André et al., 2016). To the best of our knowledge, cationized pullulan have been used for the first time to build miRNA delivery nanosystems. The obtained nanoparticles proved to be non-cytotoxic on HUVECs cells after 1 day incubation. Neither toxic reagent nor organic solvent were used. With further experiments proving the efficacy of the systems *in vivo*, we expect to contribute for the development of new safe pullulan-based delivery systems for miRNA therapeutics.

**Appendices:** Table A.1: Elemental analysis of pullulan and cationic pullulan derivatives.

#### Author Contributions:

**Fernanda C. Moraes:** Conceptualization, Methodology, Validation, Formal analysis, Investigation, Writing- Original draft preparation, Writing Review and Editing, Visualization. **Joana C. Antunes:** Conceptualization, Investigation, Writing-Review and Editing, Visualization, Supervision. **Laura Marcelo Forero Ramirez:** Conceptualization, Methodology, Investigation. **Paola Aprile:**

Methodology, Investigation. **Gregory Franck:** Methodology, Investigation. **Cédric Chauvierre:** Conceptualization, Resources, Writing-Review and Editing, Visualization, Supervision, Funding acquisition. **Frédéric Chaubet:** Conceptualization, Resources, Writing-Review and Editing, Visualization, Supervision, Project administration, Funding acquisition. **Didier Letourneur:** Conceptualization, Resources, Writing-Review and Editing, Visualization, Supervision, Project administration, Funding acquisition.

**Funding:** This work was supported by INSERM, Université de Paris and Université Paris 13. The PhD fellowship was funded by CONSELHO NACIONAL DE DESENVOLVIMENTO CIENTÍFICO E TECNOLÓGICO (CNPq) from Brazil grant number 201245/2017-5.

**Acknowledgments:** The authors are grateful to PhD fellowship for Fernanda C. Moraes from the *Conselho Nacional de Desenvolvimento Científico e Tecnológico* (CNPq). Thanks also to Camille Le Guilcher and Soraya Lanouar for assistance in data analysis.

**Conflicts of Interest:** The authors declare no conflict of interest.

## References

- Ahmed, T., Aljaeid, B., 2016. Preparation, characterization, and potential application of chitosan, chitosan derivatives, and chitosan metal nanoparticles in pharmaceutical drug delivery. *Drug Des. Devel. Ther.* 483. <https://doi.org/10.2147/DDDT.S99651>
- Alameh, M., Lavertu, M., Tran-Khanh, N., Chang, C.-Y., Lesage, F., Bail, M., Darras, V., Chevrier, A., Buschmann, M.D., 2018. siRNA Delivery with Chitosan: Influence of Chitosan Molecular Weight, Degree of Deacetylation, and Amine to Phosphate Ratio on in Vitro Silencing Efficiency, Hemocompatibility, Biodistribution, and in Vivo Efficacy. *Biomacromolecules* 19, 112–131. <https://doi.org/10.1021/acs.biomac.7b01297>
- André, E.M., Pensado, A., Resnier, P., Braz, L., Rosa da Costa, A.M., Passirani, C., Sanchez, A., Montero-Menei, C.N., 2016. Characterization and comparison of two novel nanosystems associated with siRNA for cellular therapy. *Int. J. Pharm.* 497, 255–267.

<https://doi.org/10.1016/j.ijpharm.2015.11.020>

Antunes, J.C., Benarroch, L., Moraes, F.C., Juenet, M., Gross, M.-S., Aubart, M., Boileau, C., Caligiuri, G., Nicoletti, A., Ollivier, V., Chaubet, F., Letourneur, D., Chauvierre, C., 2019. Core-Shell Polymer-Based Nanoparticles To Deliver MiR-155-5p To Endothelial Cells. *Mol. Ther. - Nucleic Acids*

370 S2162253119301465. <https://doi.org/10.1016/j.omtn.2019.05.016>

Avadi, M.R., Sadeghi, A.M.M., Mohammadpour, N., Abedin, S., Atyabi, F., Dinarvand, R., Rafiee-Tehrani, M., 2010. Preparation and characterization of insulin nanoparticles using chitosan and Arabic gum with ionic gelation method. *Nanomedicine Nanotechnol. Biol. Med.* 6, 58–63.

<https://doi.org/10.1016/j.nano.2009.04.007>

375 Bernardo, B.C., Ooi, J.Y., Lin, R.C., McMullen, J.R., 2015. miRNA therapeutics: a new class of drugs with potential therapeutic applications in the heart. *Future Med. Chem.* 7, 1771–1792.

<https://doi.org/10.4155/fmc.15.107>

Candido, S., Lupo, G., Pennisi, M., Basile, M., Anfuso, C., Petralia, M., Gattuso, G., Vivarelli, S., Spandidos, D., Libra, M., Falzone, L., 2019. The analysis of miRNA expression profiling datasets reveals inverse microRNA patterns in glioblastoma and Alzheimer's disease. *Oncol. Rep.*

380 <https://doi.org/10.3892/or.2019.7215>

Cao, Y., Tan, Y.F., Wong, Y.S., Liew, M.W.J., Venkatraman, S., 2019. Recent Advances in Chitosan-Based Carriers for Gene Delivery. *Mar. Drugs* 17, 381.

<https://doi.org/10.3390/md17060381>

385 Chakraborty, C., Sharma, A.R., Sharma, G., Doss, C.G.P., Lee, S.-S., 2017. Therapeutic miRNA and siRNA: Moving from Bench to Clinic as Next Generation Medicine. *Mol. Ther. - Nucleic Acids* 8, 132–143. <https://doi.org/10.1016/j.omtn.2017.06.005>

Cumpstey, I., 2013. Chemical Modification of Polysaccharides. ISRN Org. Chem. 2013, 1–27.

<https://doi.org/10.1155/2013/417672>

390 de Paula Pansani Oliveira, F., Picola, I.P.D., Shi, Q., Barbosa, H.F.G., de Oliveira Tiera, V.A.,  
Fernandes, J.C., Tiera, M.J., 2013. Synthesis and evaluation of diethylethylamine–chitosan for gene  
delivery: composition effects on the *in vitro* transfection efficiency. Nanotechnology 24, 055101.

<https://doi.org/10.1088/0957-4484/24/5/055101>

Devaux, Y., Stammet, P., Friberg, H., Hassager, C., Kuiper, M.A., Wise, M.P., Nielsen, N., for the  
395 Biomarker subcommittee of the TTM trial (Target Temperature Management After Cardiac Arrest,  
NCT01020916), 2015. MicroRNAs: new biomarkers and therapeutic targets after cardiac arrest? Crit.  
Care 19, 54. <https://doi.org/10.1186/s13054-015-0767-2>

Dionísio, M., Braz, L., Corvo, M., Lourenço, J.P., Grenha, A., Rosa da Costa, A.M., 2016. Charged  
pullulan derivatives for the development of nanocarriers by polyelectrolyte complexation. Int. J. Biol.  
400 Macromol. 86, 129–138. <https://doi.org/10.1016/j.ijbiomac.2016.01.054>

Falzone, Lupo, Rosa, Crimi, Anfuso, Salemi, Rapisarda, Libra, Candido, 2019. Identification of Novel  
MicroRNAs and Their Diagnostic and Prognostic Significance in Oral Cancer. Cancers 11, 610.  
<https://doi.org/10.3390/cancers11050610>

Ganas, C., Weiß, A., Nazarenius, M., Rösler, S., Kissel, T., Rivera\_Gil, P., Parak, W.J., 2014.  
405 Biodegradable capsules as non-viral vectors for in vitro delivery of PEI/siRNA polyplexes for efficient  
gene silencing. J. Controlled Release 196, 132–138. <https://doi.org/10.1016/j.jconrel.2014.10.006>

Gary, D.J., Puri, N., Won, Y.-Y., 2007. Polymer-based siRNA delivery: Perspectives on the  
fundamental and phenomenological distinctions from polymer-based DNA delivery. J. Controlled  
Release 121, 64–73. <https://doi.org/10.1016/j.jconrel.2007.05.021>



- 410 Gaur, S., Wen, Y., Song, J.H., Parikh, N.U., Mangala, L.S., Blessing, A.M., Ivan, C., Wu, S.Y.,  
Varkaris, A., Shi, Y., Lopez-Berestein, G., Frigo, D.E., Sood, A.K., Gallick, G.E., 2015. Chitosan  
nanoparticle-mediated delivery of miRNA-34a decreases prostate tumor growth in the bone and its  
expression induces non-canonical autophagy. *Oncotarget* 6.  
<https://doi.org/10.18632/oncotarget.4971>
- 415 Goyal, R., Kapadia, C.H., Melamed, J.R., Riley, R.S., Day, E.S., 2018. Layer-by-Layer Assembled  
Gold Nanoshells for the Intracellular Delivery of miR-34a. *Cell. Mol. Bioeng.* 11, 383–396.  
<https://doi.org/10.1007/s12195-018-0535-x>
- Hou, W., Tian, Q., Steuerwald, N.M., Schrum, L.W., Bonkovsky, H.L., 2012. The let-7 microRNA  
enhances heme oxygenase-1 by suppressing Bach1 and attenuates oxidant injury in human  
420 hepatocytes. *Biochim. Biophys. Acta BBA - Gene Regul. Mech.* 1819, 1113–1122.  
<https://doi.org/10.1016/j.bbagr.2012.06.001>
- Karimi, M., Avci, P., Ahi, M., Gazori, T., Hamblin, M.R., Naderi-Manesh, H., 2013. Evaluation of  
Chitosan-Tripolyphosphate Nanoparticles as a p-shRNA Delivery Vector: Formulation, Optimization  
and Cellular Uptake Study. *J. Nanopharmaceutics Drug Deliv.* 1, 266–278.  
425 <https://doi.org/10.1166/jnd.2013.1027>
- K.R., S., V., P., 2017. Review on production, downstream processing and characterization of  
microbial pullulan. *Carbohydr. Polym.* 173, 573–591. <https://doi.org/10.1016/j.carbpol.2017.06.022>
- Lächelt, U., Wagner, E., 2015. Nucleic Acid Therapeutics Using Polyplexes: A Journey of 50 Years  
(and Beyond). *Chem. Rev.* 115, 11043–11078. <https://doi.org/10.1021/cr5006793>
- 430 Li, Q., Tan, W., Zhang, C., Gu, G., Guo, Z., 2016. Synthesis of water soluble chitosan derivatives with  
halogeno-1,2,3-triazole and their antifungal activity. *Int. J. Biol. Macromol.* 91, 623–629.

<https://doi.org/10.1016/j.ijbiomac.2016.06.006>

Liu, P., Meng, W., Wang, S., Sun, Y., Aqeel Ashraf, M., 2015. Quaternary ammonium salt of chitosan: preparation and antimicrobial property for paper. *Open Med.* 10.

435 <https://doi.org/10.1515/med-2015-0081>

Liu, X., Howard, K.A., Dong, M., Andersen, M.Ø., Rahbek, U.L., Johnsen, M.G., Hansen, O.C., Besenbacher, F., Kjems, J., 2007. The influence of polymeric properties on chitosan/siRNA nanoparticle formulation and gene silencing. *Biomaterials* 28, 1280–1288.

<https://doi.org/10.1016/j.biomaterials.2006.11.004>

440 Lounis, F.M., Chamieh, J., Gonzalez, P., Cottet, H., Leclercq, L., 2016. Prediction of Polyelectrolyte Complex Stoichiometry for Highly Hydrophilic Polyelectrolytes. *Macromolecules* 49, 3881–3888.

<https://doi.org/10.1021/acs.macromol.6b00463>

Mao, S., Sun, W., Kissel, T., 2010. Chitosan-based formulations for delivery of DNA and siRNA. *Adv. Drug Deliv. Rev.* 62, 12–27. <https://doi.org/10.1016/j.addr.2009.08.004>

445 Nuhn, L., Tomcin, S., Miyata, K., Mailänder, V., Landfester, K., Kataoka, K., Zentel, R., 2014. Size-Dependent Knockdown Potential of siRNA-Loaded Cationic Nanohydrogel Particles. *Biomacromolecules* 15, 4111–4121. <https://doi.org/10.1021/bm501148y>

Patil, S.D., Rhodes, D.G., Burgess, D.J., 2005. DNA-based therapeutics and DNA delivery systems: A comprehensive review. *AAPS J.* 7, E61–E77. <https://doi.org/10.1208/aapsj070109>

450 Poddar, S., Kesharwani, D., Datta, M., 2019. miR-449a regulates insulin signalling by targeting the Notch ligand, Jag1 in skeletal muscle cells. *Cell Commun. Signal.* 17. <https://doi.org/10.1186/s12964-019-0394-7>

Prajapati, V.D., Jani, G.K., Khanda, S.M., 2013. Pullulan: An exopolysaccharide and its various

applications. Carbohydr. Polym. 95, 540–549. <https://doi.org/10.1016/j.carbpol.2013.02.082>

455 Qiagen, 2018. Guidelines for miRNA mimic and miRNA inhibitor experiments.

<https://www.qiagen.com/fr/resources/resourcedetail?id=3e1477ad-74a2-4ee6-9c31->

54b1997f2941&lang=en.

Ragelle, H., Riva, R., Vandermeulen, G., Naeye, B., Pourcelle, V., Le Duff, C.S., D'Haese, C., Nysten,

B., Braeckmans, K., De Smedt, S.C., Jérôme, C., Préat, V., 2014. Chitosan nanoparticles for siRNA

460 delivery: Optimizing formulation to increase stability and efficiency. J. Controlled Release 176, 54–63.

<https://doi.org/10.1016/j.jconrel.2013.12.026>

Rekha, M.R., Sharma, C.P., 2009. Blood compatibility and in vitro transfection studies on cationically

modified pullulan for liver cell targeted gene delivery. Biomaterials 30, 6655–6664.

<https://doi.org/10.1016/j.biomaterials.2009.08.029>

465 Rupaimoole, R., Slack, F.J., 2017. MicroRNA therapeutics: towards a new era for the management of

cancer and other diseases. Nat. Rev. Drug Discov. 16, 203–222.

<https://doi.org/10.1038/nrd.2016.246>

San Juan, A., Bala, M., Hlawaty, H., Portes, P., Vranckx, R., Feldman, L.J., Letourneur, D., 2009.

Development of a Functionalized Polymer for Stent Coating in the Arterial Delivery of Small

470 Interfering RNA. Biomacromolecules 10, 3074–3080. <https://doi.org/10.1021/bm900740g>

San Juan, A., Ducrocq, G., Hlawaty, H., Bataille, I., Guénin, E., Letourneur, D., Feldman, L.J., 2007.

Tubular cationized pullulan hydrogels as local reservoirs for plasmid DNA. J. Biomed. Mater. Res. A

83A, 819–827. <https://doi.org/10.1002/jbm.a.31413>

Scholz, C., Wagner, E., 2012. Therapeutic plasmid DNA versus siRNA delivery: Common and

475 different tasks for synthetic carriers. J. Controlled Release 161, 554–565.

<https://doi.org/10.1016/j.jconrel.2011.11.014>

Shao, Z., Xu, T., Wang, S., Liu, W., 2014. Elucidating the role of free polycationic chains in polycation gene carriers by free chains of polyethylenimine or N,N,N-trimethyl chitosan plus a certain polyplex.

Int. J. Nanomedicine 3231. <https://doi.org/10.2147/IJN.S64308>

480 Shen, Z., Xia, Y., Yang, Q., Tian, W., Chen, K., Ma, Y., 2017. Polymer–Nucleic Acid Interactions. Top. Curr. Chem. 375, 44. <https://doi.org/10.1007/s41061-017-0131-x>

Shi, B., Zheng, M., Tao, W., Chung, R., Jin, D., Ghaffari, D., Farokhzad, O.C., 2017. Challenges in DNA Delivery and Recent Advances in Multifunctional Polymeric DNA Delivery Systems. Biomacromolecules 18, 2231–2246. <https://doi.org/10.1021/acs.biomac.7b00803>

485 Stefan, J., Kus, K., Wisniewska, A., Kaminski, K., Szczubialka, K., Jawien, J., Nowakowska, M., Korbut, R., 2016. New cationically modified pullulan attenuates atherogenesis and influences lipid metabolism in apoE-knockout mice. J Physiol Pharmacol 67, 739–749.

Stuart, B.H., 2004. Infrared Spectroscopy: Fundamentals and Applications 208.

Tekie, F.S.M., Atyabi, F., Soleimani, M., Arefian, E., Atashi, A., Kiani, M., Khoshayand, M.R., Amini,

490 M., Dinarvand, R., 2015. Chitosan polyplex nanoparticle vector for miR-145 expression in MCF-7: Optimization by design of experiment. Int. J. Biol. Macromol. 81, 828–837. <https://doi.org/10.1016/j.ijbiomac.2015.09.014>

Thanou, M., Florea, B.I., Geldof, M., Junginger, H.E., Borchard, G., 2002. Quaternized chitosan oligomers as novel gene delivery vectors in epithelial cell lines. Biomaterials 23, 153–159.

495 [https://doi.org/10.1016/S0142-9612\(01\)00090-4](https://doi.org/10.1016/S0142-9612(01)00090-4)

van Rooij, E., Marshall, W.S., Olson, E.N., 2008. Toward MicroRNA–Based Therapeutics for Heart Disease: The Sense in Antisense. Circ. Res. 103, 919–928.

<https://doi.org/10.1161/CIRCRESAHA.108.183426>

Vauthier, C., Zandanel, C., Ramon, A.L., 2013. Chitosan-based nanoparticles for in vivo delivery of  
500 interfering agents including siRNA. *Curr. Opin. Colloid Interface Sci.* 18, 406–418.

<https://doi.org/10.1016/j.cocis.2013.06.005>

Wang, S., Cao, M., Deng, X., Xiao, X., Yin, Z., Hu, Q., Zhou, Z., Zhang, F., Zhang, R., Wu, Y., Sheng,  
W., Zeng, Y., 2015. Degradable Hyaluronic Acid/Protamine Sulfate Interpolyelectrolyte Complexes  
as miRNA-Delivery Nanocapsules for Triple-Negative Breast Cancer Therapy. *Adv. Healthc. Mater.*  
505 4, 281–290. <https://doi.org/10.1002/adhm.201400222>

Wolff JA, Malone RW, Williams P, Chong W, Acsadi G, Jani A, Felgner PL, 1990. Direct gene transfer  
into mouse muscle in vivo. *Science* 247, 1465–1468.

Wu, D., Delair, T., 2015. Stabilization of chitosan/hyaluronan colloidal polyelectrolyte complexes in  
physiological conditions. *Carbohydr. Polym.* 119, 149–158.  
510 <https://doi.org/10.1016/j.carbpol.2014.11.042>

Xiong, Q., Lee, G.Y., Ding, J., Li, W., Shi, J., 2018. Biomedical applications of mRNA nanomedicine.  
*Nano Res.* 11, 5281–5309. <https://doi.org/10.1007/s12274-018-2146-1>

Zarghampoor, F., Azarpira, N., Khatami, S.R., Behzad-Behbahani, A., Foroughmand, A.M., 2019.  
Improved translation efficiency of therapeutic mRNA. *Gene* 707, 231–238.  
515 <https://doi.org/10.1016/j.gene.2019.05.008>

Zhao, Q.-Q., Chen, J.-L., Lv, T.-F., He, C.-X., Tang, G.-P., Liang, W.-Q., Tabata, Y., Gao, J.-Q., 2009.  
N/P Ratio Significantly Influences the Transfection Efficiency and Cytotoxicity of a  
Polyethylenimine/Chitosan/DNA Complex. *Biol. Pharm. Bull.* 32, 706–710.  
<https://doi.org/10.1248/bpb.32.706>

520 Zhu, L., Chen, T., Ye, W., Wang, J.-Y., Zhou, J.-P., Li, Z.-Y., Li, C.-C., 2019. Circulating miR-182-5p and miR-5187-5p as biomarkers for the diagnosis of unprotected left main coronary artery disease. J. Thorac. Dis. 11, 1799–1808. <https://doi.org/10.21037/jtd.2019.05.24>

## Figure Legends

525 **Figure 1.** Schematic representation of synthesis route for alkylation of pullulan using glycidyltrimethylammonium chloride (GTMAC).

**Figure 2.** FTIR spectra of (a) non-modified pullulan and (b) QA-pullulan.

**Figure 3.** <sup>1</sup>H-NMR spectra of (a) non-modified pullulan and (b) QA-pullulan in D<sub>2</sub>O. 1A, 1B, 1C signals depicted anomeric H from maltotriose base unit of pullulan. Numbers 2-6 corresponded to H on anhydroglucose unit. H from GTMAC substituent (b) were depicted with numbers from 7 to 10.

530

**Figure 4.** Cytocompatibility of (a) non-modified pullulan and (b) QA-pullulan towards HUVECs at 200, 500 and 1,000 µg/mL after 24, 48 and 72h of incubation. Results are shown as mean ± SD from 3 independent experiments with no statistical differences detected using the Wilcoxon matched-pairs signed rank test.

**Figure 5.** Schematic representation of preparation of QA-pullulan/miRNA polyplexes by electrostatic interactions.

535

**Figure 6.** Physico-chemical characterization of QA-pullulan/miRNA polyplexes: (a) Size distribution from Light Scattering (LS) expressed by intensity and number percentages; (b) Morphology of polyplexes obtained by TEM microscopy; (c) Size (nm), Pdl, attenuator and count rate values measured by LS and zeta potential (mV) measured by Doppler laser electrophoresis. Results are shown as mean ± standard deviation of 3 different samples.

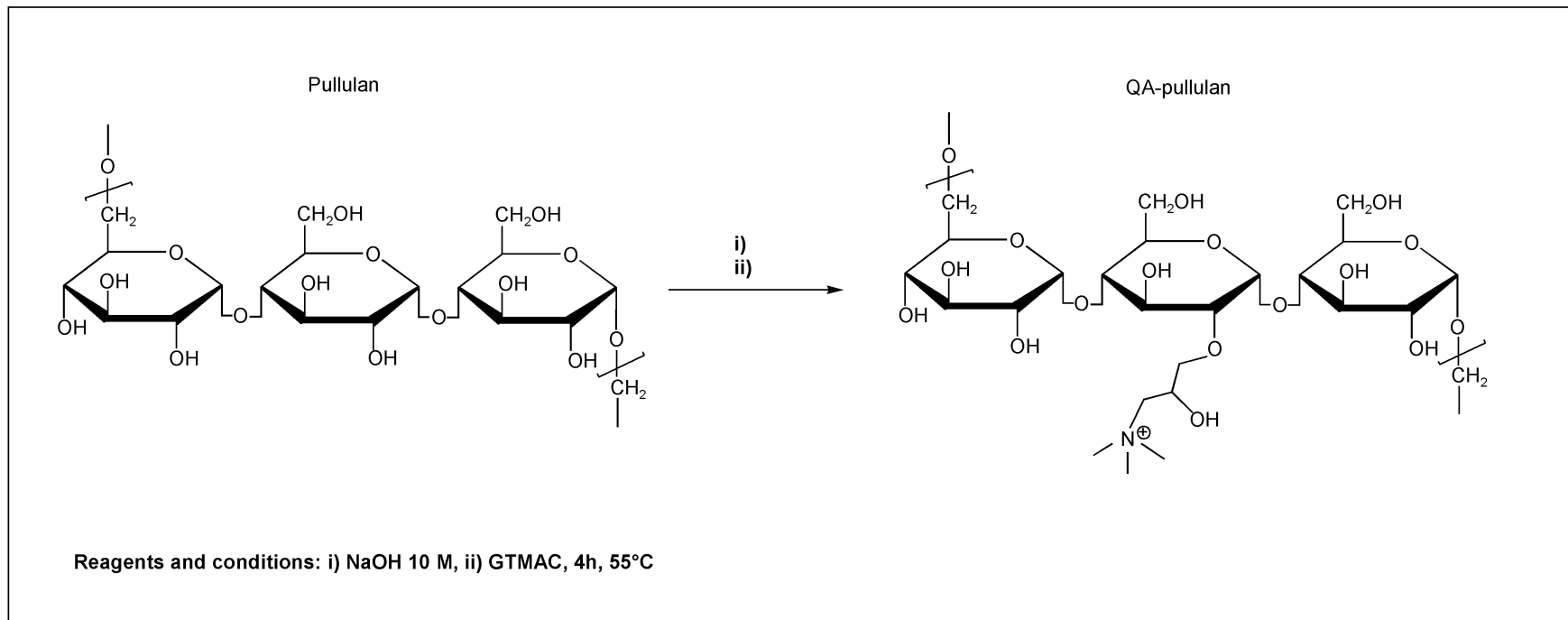
540

**Figure 7.** (a) miRNA presence onto polyplexes after miRNA desorption confirmed by agarose gel electrophoresis using an Ultra-Low Range GeneRuler DNA Ladder (10-300 bp) as control and RNA amount (ng) quantified by the intensity of the band when compared to miRNA alone (0.04 mg/mL, 9 µL) using ImageJ software; (b) RNA amount (ng/µL) quantified by UV absorbance (n=3).

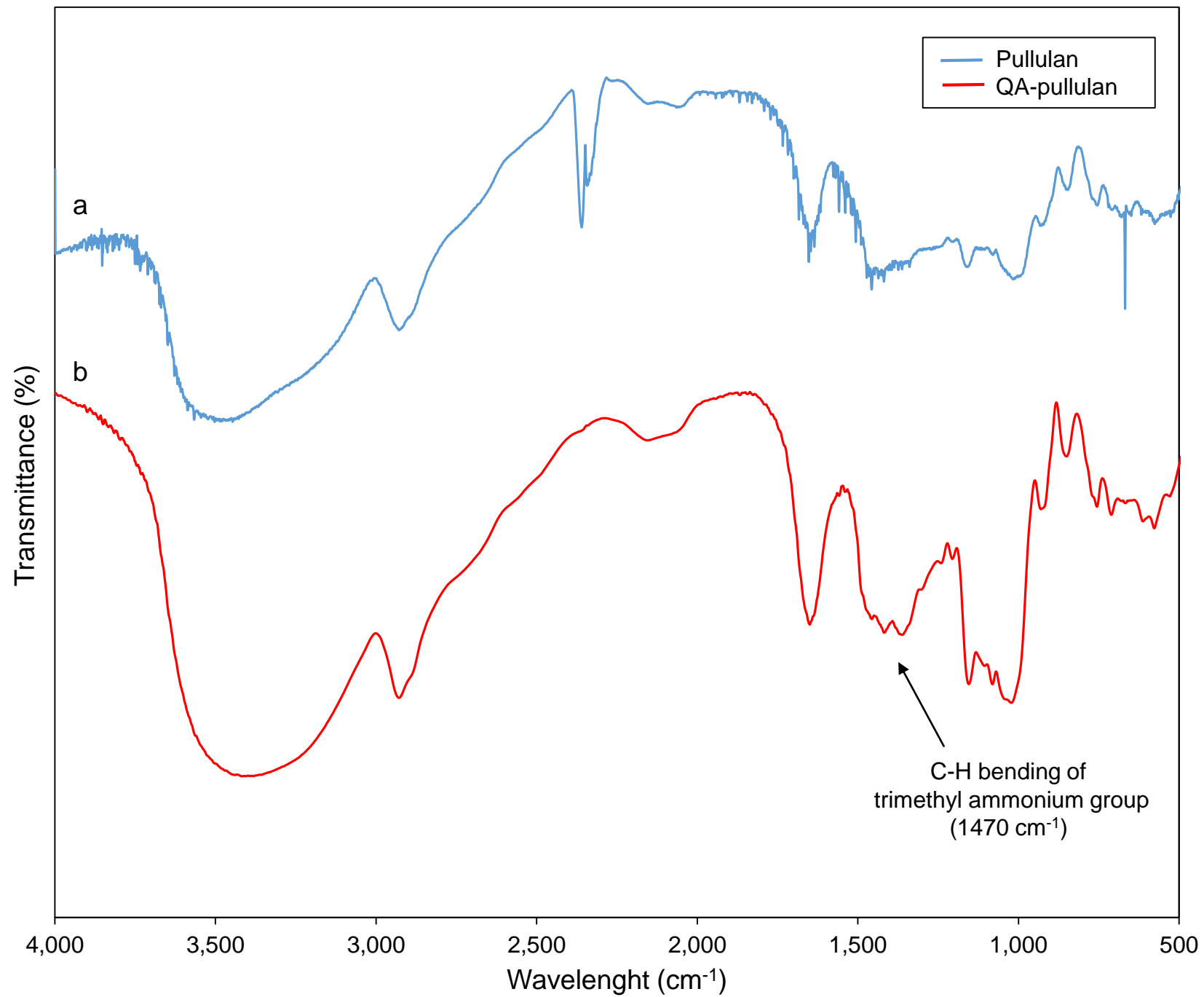
545 **Figure 8.** Stability of QA-pullulan/miRNA polyplexes evaluated by size (left) and Pdl evolution (right) measured by Light Scattering as function of time of incubation in water at 4°C (mean ± SD, n=3).

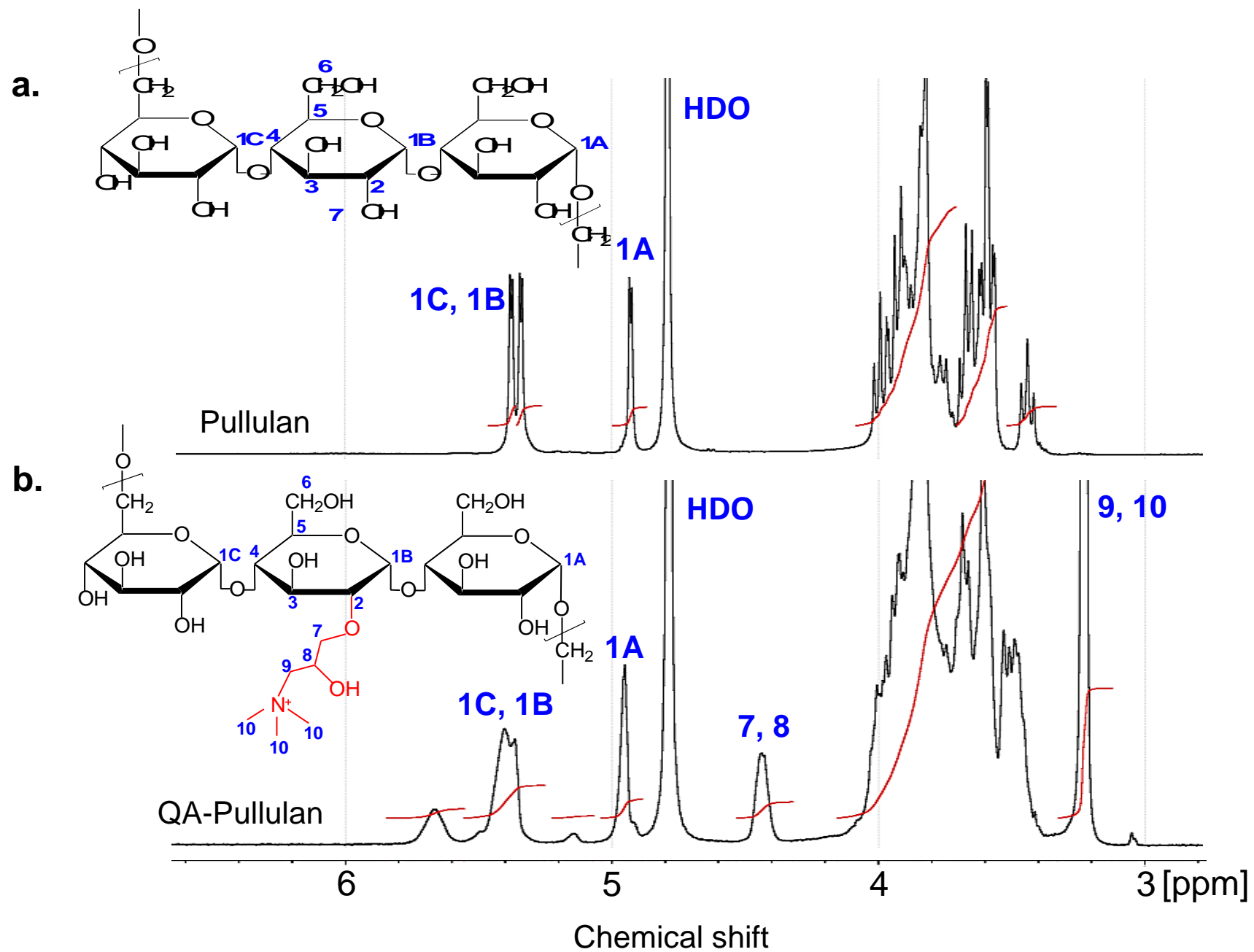
**Figure 9. (a)** Cytocompatibility of complexes towards HUVECs exposed to increasing concentrations of QA-pullulan/miRNA polyplexes measured by resazurin conversion after 1 day of incubation. Results are shown as mean  $\pm$  SD from 3 independent experiments with no statistical differences detected using the Wilcoxon matched-pairs signed rank test. **(b)** Optical images of confluent cells without polyplexes and with 100  $\mu$ g/mL and 200  $\mu$ g/mL of polyplexes. Scale bar corresponds to 200  $\mu$ m.

**Figure 10.** Fluorescence microscopy images of HUVECs evidencing miRNA delivery. Left column: cells' nuclei stained with DAPI (depicted in blue); middle column: FAM labelled miRNA (depicted in green); right column: merged images. **(A)** without treatment, **(B)** cells treated with FAM-labelled miRNA, **(C)** cells treated with FAM-labelled miRNA in presence of unmodified pullulan; **(D)** cells treated with polyplexes formed by FAM-labelled miRNA and QA-pullulan including Z-stack-assembled fluorescence images (zoom). Treatments were performed for 30 min at 37°C. Scale bar: 20  $\mu$ m.

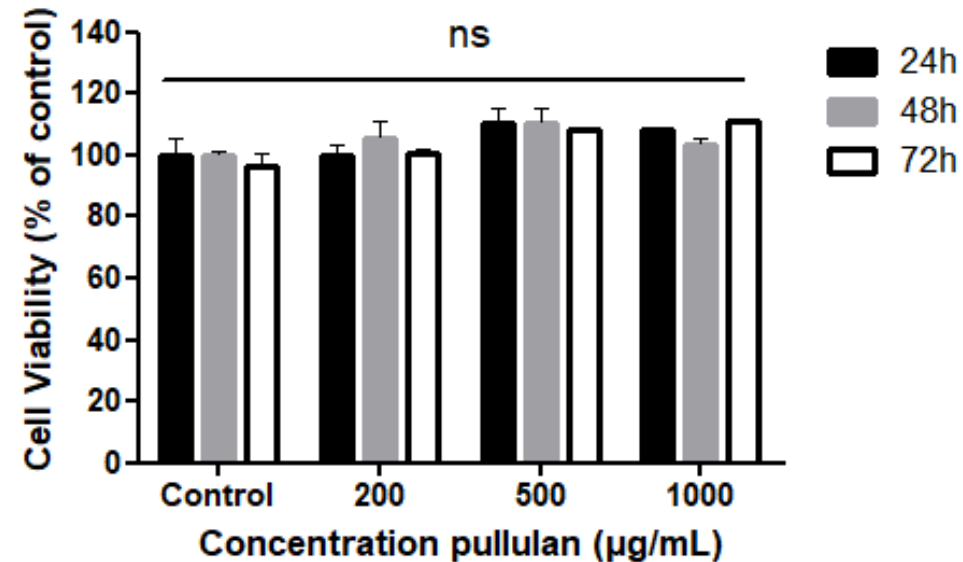




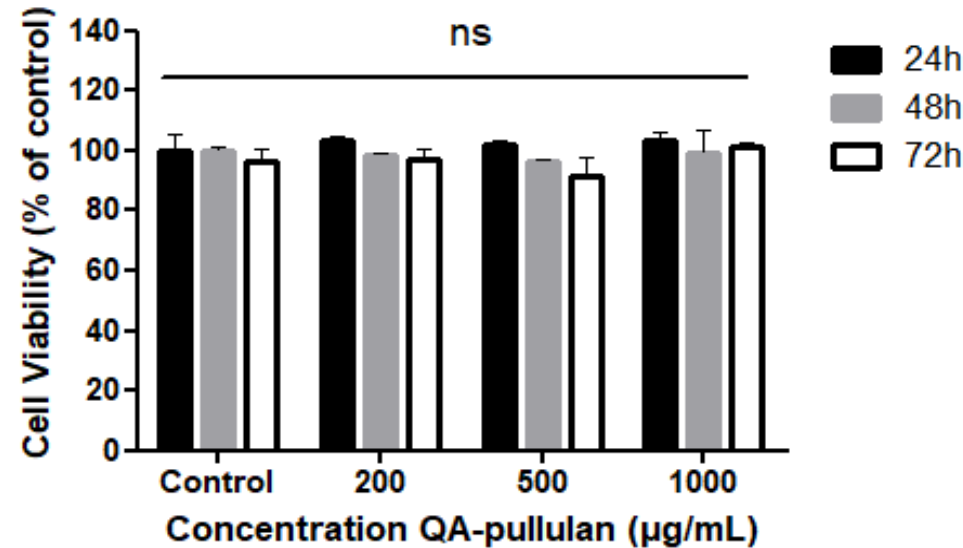


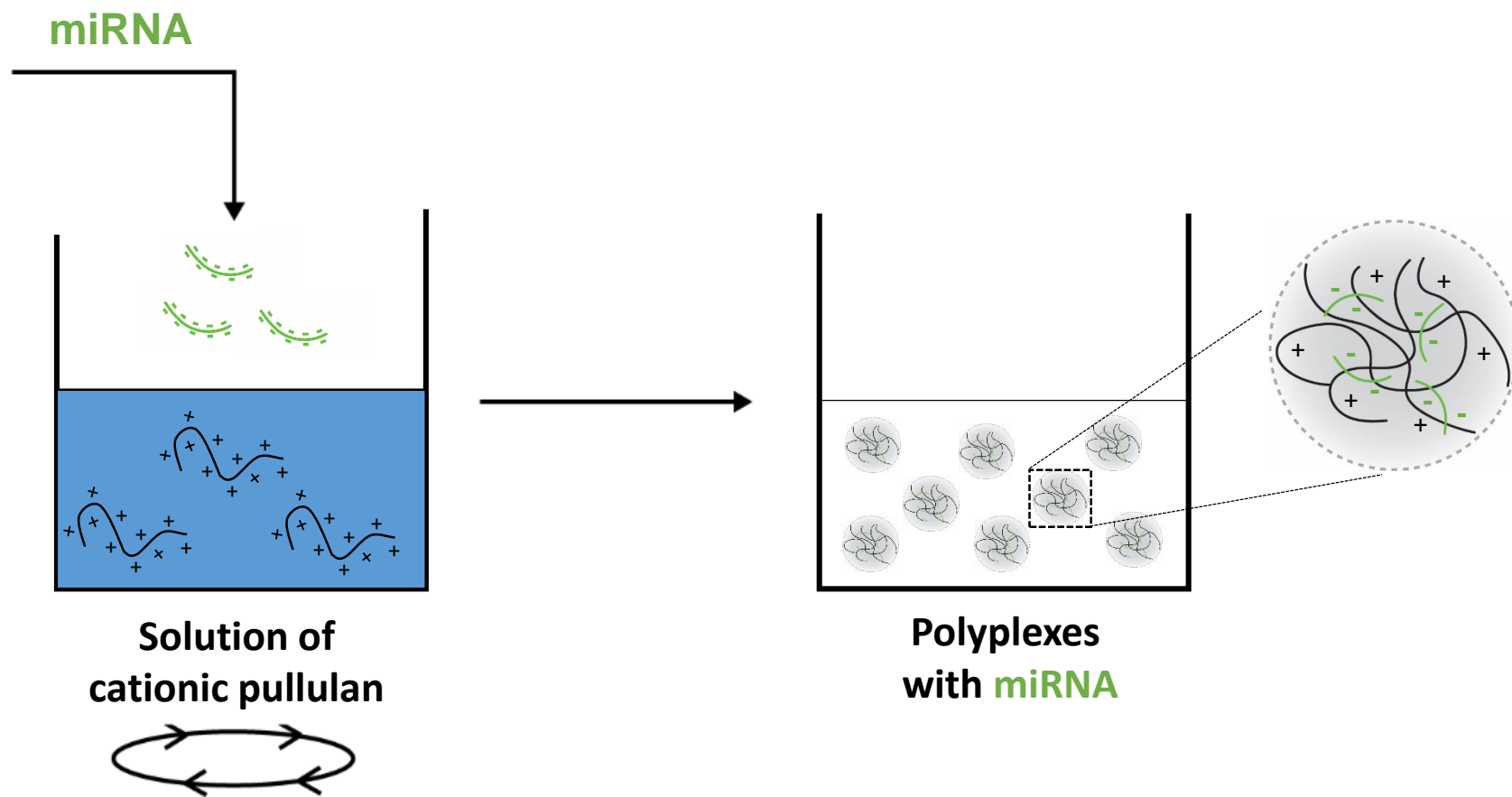


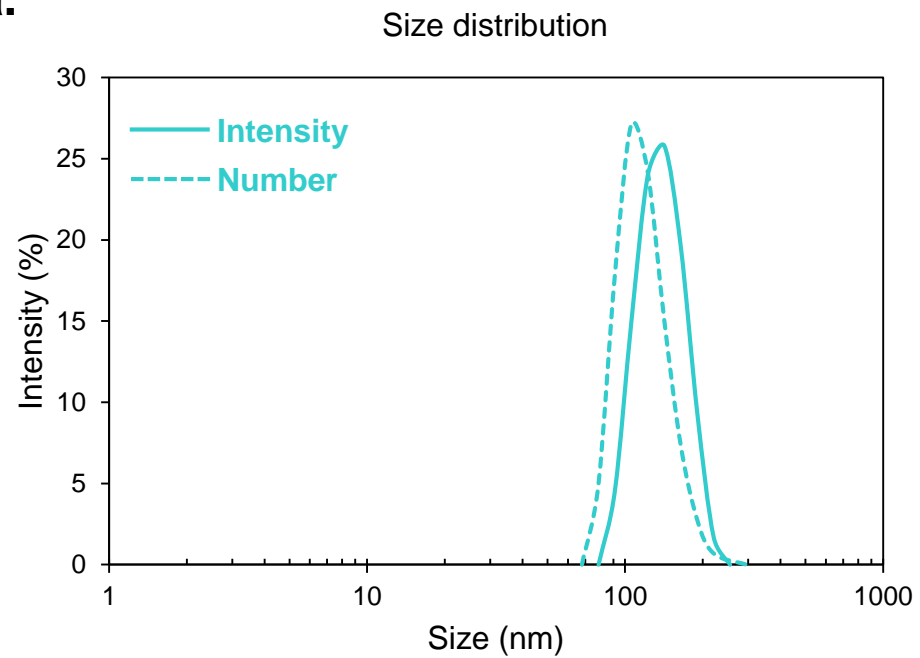
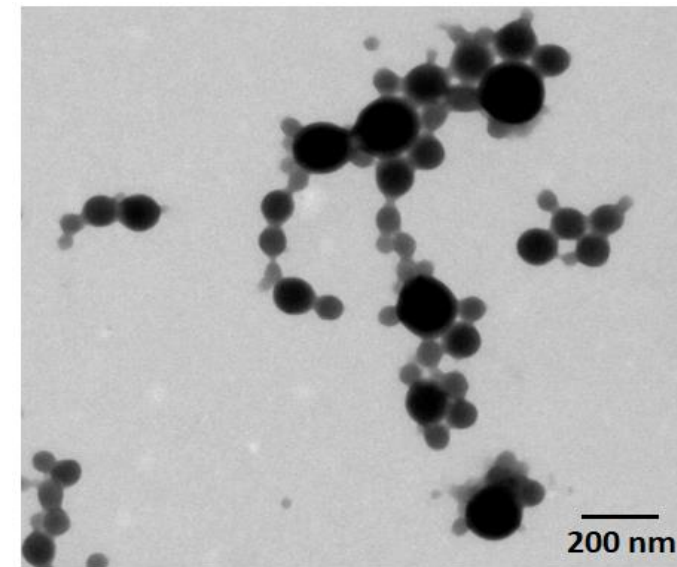
a.



b.

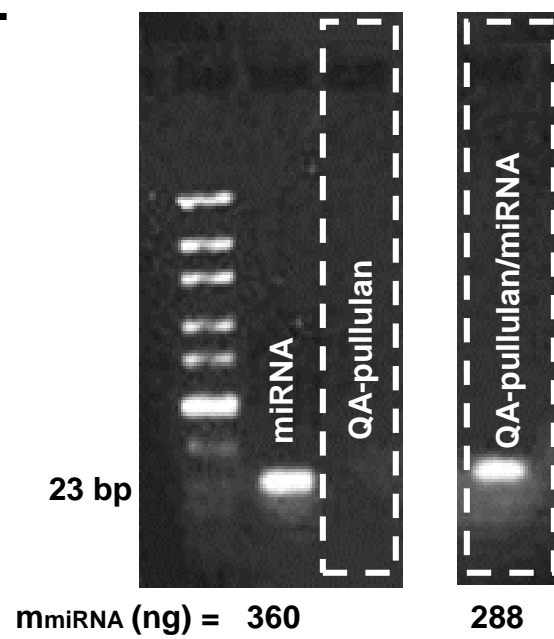




**a.****b.****c.**

Size (nm)	PdI	Attenuator	Count rate (kcps)	$\zeta$ potential (mV)
133 $\pm$ 30	0.07 $\pm$ 0.04	7	178	-12 $\pm$ 5

**a.**



**b.**

